# Spatial Variability of Ozigo Wood Beams under Long-Term Loadings in Various Environmental Exposures

Valérie Nsouami, Nicaise Manfoumbi, Rostand Moutou Pitti, Emilio Bastidas-Arteaga

*Article*

# Spatial Variability of Ozigo Wood Beams under Long-Term Loadings in Various Environmental Exposures

Valérie Nsouami [1], Nicaise Manfoumbi [2], Rostand Moutou Pitti [3,4] and Emilio Bastidas-Arteaga [5,*]

[1] Ecole Normale Supérieure L'Enseignement Technique (ENSET), LaReVa Bois, BP 3989 Libreville, Gabon; nsouamijeanj@gmail.com
[2] Ecole Polytechnique de Masuku, Université des Sciences et Techniques de Masuku, BP 901 Franceville, Gabon; nicaise.manfoumbi@gmail.com
[3] Clermont Auvergne INP, CNRS, Institut Pascal, Université Clermont Auvergne, BP 10448, 63000 Clermont-Ferrand, France; rostand.moutou_pitti@uca.fr
[4] CENAREST, IRT, BP 14070 Libreville, Gabon
[5] Laboratoire des Sciences de l'Ingénieur pour l'Environnement (LaSIE UMR CNRS 7356), La Rochelle Université, 17042 La Rochelle, France
* Correspondence: ebastida@univ-lr.fr

**Abstract:** Timber is a renewable material that should be more used for sustainable construction. While the mechanical behavior and durability of some species have been widely studied in the past, few studies are available for the Ozigo (*Dacryodes buettneri*) specie. This paper deals with the spatial variability of Ozigo beams subjected to long-term loadings and different environmental conditions. These beams were previously subjected to long-term creep in three environments (air-conditioned, unsheltered, and sheltered) at Masuku in the south-east of Gabon. Various specimens were extracted from these beams to determine its moisture content and subjected to three-point bending tests to obtain the modulus of elasticity and failure stress at various points in the space. The results obtained showed that, after long-term loadings, environmental exposure combined with mechanical loading, play a key role in the mechanical properties of the timber beams. A reduction of strength was found for the specimens extracted from the unsheltered and sheltered outdoor exposures in comparison with those extracted from the air-conditioned exposure. Concerning the spatial variability, statistical tests confirm that there is significant spatial correlation. It was also found that the spatial variation of properties in the beam is not stationary because it was affected by loading and support conditions.

**Keywords:** Ozigo (*Dacryodes buettneri*); timber; spatial variability; environmental effects; mechanical properties; creep

## 1. Introduction

In tropical countries such as Gabon, the forest covers more than 80% of the territory with about 480 various types of species. To diversify its economy, the Gabonese government decided to ban the export of logs from January 2010, thus paving the way for local processing into finished products and promotion of this sustainable resource in the construction of timber structures that are characterized by a low environmental footprint [1–4]. Predicting structural responses and estimating the durability of tropical timber structures subjected to thermo-hygro-mechanical loading [5] appears as an important challenge for promoting its use in the construction sector, especially for the Ozigo species (*Dacryodes buettneri*) which is an endemic species after Okume (*Aucoumea klaineana Pierre*). The Ozigo specie is a leafy tree of tropical origin from western Central Africa (Gabon and other equatorial countries). This specie is mainly used for plywood construction, in veneer, and finished or semi-finished products [6].

The mechanical behavior of timber structures depends strongly on climate variations [7]. With over 1900 mm of annual precipitation, around 85% relative humidity and a

mean temperature near 27 °C, the environmental conditions in Gabon are very arduous and impact the durability of timber structures during its service life [8]. Therefore, these environmental conditions should be considered in the design of wooden structures to ensure adequate levels of serviceability and safety, especially for structures exposed in tropical environments. In addition, there is a variability of mechanical parameters due to the heterogeneous character of wood material that depends on the age, location of wood in the tree, loading time [9,10], climatic conditions [11,12], nodes, growth of annual rings [13,14], etc. This variability is both random and spatially distributed and is commonly called 'spatial variability' [15,16].

In the literature background, several authors investigated the spatial variability of materials [17]. Some of them developed statistical and mathematical models, based on random field tools, to characterize, to represent or to propagate it. For example, Clerc et al. [18] and Rakotovao Ravahatra et al. [19] proposed procedures for characterizing the spatial variability from one-dimensional discrete data. Both studies were applied to reinforced concrete structures. The outcomes of these studies could be used to represent the spatial variability using several methods such as the Karhunen-Lòeve expansion, the optimal linear estimation method and/or Expansion Optimal Linear Estimation [20,21]. A detailed overview of these methods is provided by Ghanem and Spanos [22] and Sudret and Der Kiureghian [23]. The application of the outcomes and methods mentioned previously allow estimating the influence of spatial variability on safety of structures. Stewart [24] discussed about the spatial variability of damage and evaluated the related maintenance costs for the corroding reinforced concrete structures. This study highlighted the importance of considering the spatial variability to accurately estimate the probability of deteriorating structural components. Zhu et al. [25] also found that neglecting the spatial variability of reinforced concrete properties leads to an overestimation of the probability of compression failure.

Few works have been focused on the spatial variability of timber structures. Moshtaghin et al. [13,26] performed an experimental characterization of the longitudinal mechanical properties (elastic modulus and compressive strength) of light wood at different scales. They found that the dimension of the specimens should be carefully selected to avoid scale effects. A specific procedure to correct these scale effects was proposed by the authors; this fact should be accounted for when the size of the specimen is very small in comparison to the correlation length. Tran et al. [27] proposed a framework based on Bayesian networks to study the effect of the spatial variability of decay on the durability of timber beams. This framework could be used to evaluate the durability condition of the beam using partial observations; however, the spatial variability of mechanical properties was not considered in this work.

The main objective of this study is to analyze the variability and the spatial variability of mechanical properties (modulus of elasticity (MOE) and failure stress (FS)) of Ozigo beams exposed to various long-term environmental conditions and mechanical loading. Towards this aim, the beams were previously subjected to long-term creep (9 years) under three environments (air-conditioned environment, unsheltered outdoor environment, and sheltered outdoor environment) at the south-east of Gabon [28]. In addition, this study also evaluates the effects of climatic and hydric parameters on the mechanical properties of wood subjected to different environmental conditions.

This long-term work will address the crucial need to promote the sustainable development and use of wood-based materials and structures in Gabon and in the region. The study also responds to the practical need to adapt the Eurocode 5 for the design and verification of timber constructions in a tropical environment. In the mid-term, the main findings of this paper will contribute to a wider use of this renewable and sustainable material in the construction sector.

## 2. Materials and Methods

### 2.1. Materials

Ozigo is the tropical specie considered in this work. It has a light brown color and is a light wood with a density of 0.59 tons/m$^3$ ± 0.05 [29,30]. The specimens were extracted from three wood beams (89 × 176 × 3090 mm$^3$) previously subjected to a creep test in tropical atmospheres from three environments during 5 years, Figure 1 [28]. After the 5 years of loading, the beams were unloaded and remained exposed to their same environmental conditions over 3 years (recovery period) before being stored. Any treatment against decay was applied to study the natural durability of Ozigo beams under realistic exposure conditions; however, any presence of fungi or insects was observed after the exposure time. For the beams exposed outdoors, they were subjected to the rain and therefore to shrinkage swelling; however, this exposure has not generated cracks of the beams.



**Figure 1.** (**a**) Air-conditioned environment. (**b**) Unsheltered outdoor environment. (**c**) Sheltered outdoor environment.

The beams were sawn into nine sections 340 mm long. Figure 2 shows the section of the beam and the exact location of each specimen extracted in the beams. These sections were subdivided into three zones in height (upper zone (UZ), middle zone (MZ), and lower (LZ)), Figure 2a,b. From each section were extracted: two specimens for bending test, two for tensile tests and four for compression tests. Note that this paper only presents and analyses the results from the three-point bending tests (81 samples of section 15 × 15 mm$^2$ and 300 mm long). The specimens concerned by bending tests are shown in Figure 2b and the real samples are presented in Figure 2c. Before loading the specimens, the mechanical behavior of wood inside each beam cannot vary. However, after long-term loading, the upper and tensile zones are in compressive and tensile areas, respectively. Consequently, specimens in each zone will be submitted to similar mechanical conditions during the tests.
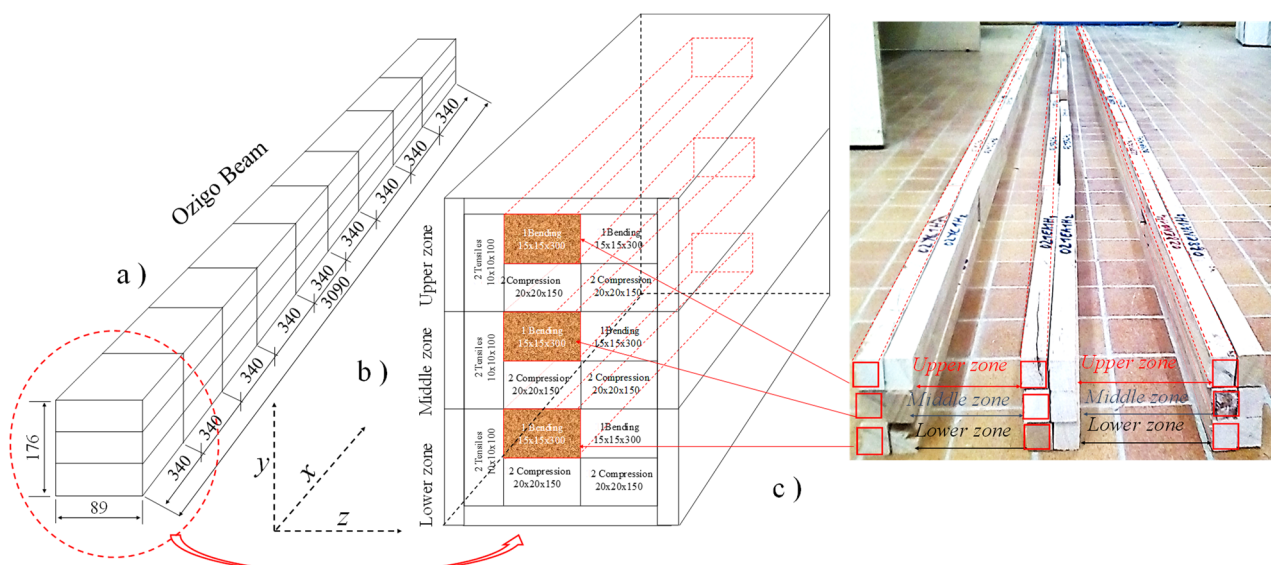


**Figure 2.** Spatial representation of the beam: (**a**) Beam cutting plane. (**b**) Arrangement of specimens in a section of the beam. (**c**) Cross-section of the specimens from the three environments.

Figure 3 presents the experimental devices used to measure the geometry, moisture content and temperature of each specimen. These devices are: (i) a caliper (Figure 3a) for measuring the dimensions; (ii) a Romus Mini 93250 brand spiked moisture meter (Figure 3b) for determining the moisture content; and (iii) a thermo-hygrometer brand Testo 510 (Figure 3c) for estimating the temperature and relative humidity during the tests. All measurements were carried out before each bending test.
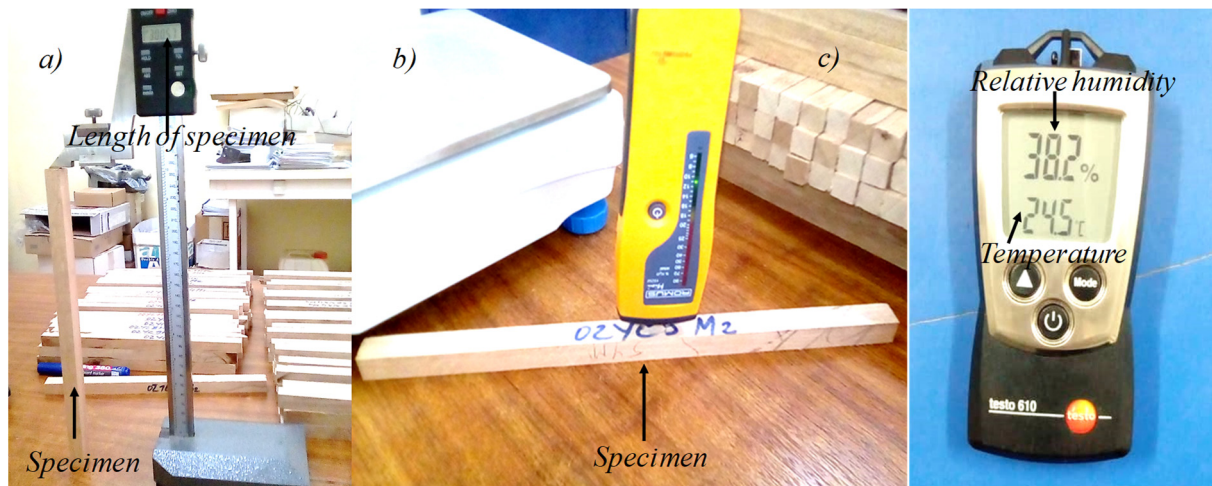


**Figure 3.** (**a**) Height caliper. (**b**) Moisture meter. (**c**) Thermo-hygrometer.

Table 1 provides the number of specimens, and the average density and moisture content per zone. At least 8 specimens per zone and 26 specimens per beam are used herein. The average values of density and moisture content provided in Table 1 illustrate the variability of these parameters for the considered beam zones and environmental exposure conditions. However, since the coefficient of variation of the density is very small (about 3%), the statistical and spatial variability analyses will only focus on the moisture content and mechanical parameters.

**Table 1.** Number of specimens per beam and average density and moisture content per zones.

| Exposure | Zone | Number of Specimens | Density (kg/m$^3$) | Moisture Content (%) |
|---|---|---|---|---|
| Air-conditioned | Upper | 8 | 580.28 | 10.08 |
| | Middle | 9 | 586.37 | 10.59 |
| | Lower | 9 | 597.96 | 10.77 |
| | Average per beam | – | 588.20 | 10.5 |
| Unsheltered | Upper | 8 | 558.15 | 8.91 |
| | Middle | 9 | 586.58 | 8.96 |
| | Lower | 9 | 583.04 | 8.92 |
| | Average per beam | – | 576.61 | 8.9 |
| Sheltered outdoor | Upper | 9 | 577.68 | 10.27 |
| | Middle | 9 | 595.33 | 10.58 |
| | Lower | 8 | 582.44 | 10.42 |
| | Average per beam | – | 585.25 | 10.4 |

Table 2 provides the average exposure conditions (temperature T, relative humidity RH) and the moisture content at the beginning of the exposure [28]. Based on the moisture content, we note that the original beams were loaded in a wet state (semi-dry and commercially dry wood), and thus dried under loading. By comparing the average values and standard deviation of the three exposures, it is observed that the temperature and

relative humidity are lower for the air-conditioned exposure; but these parameters are very close for the unsheltered and sheltered conditions. Therefore, the main difference between unsheltered and sheltered conditions will be related to the exposure to rain and sun radiation for the unsheltered condition. Indeed, the exposure of the beams to rain and sun increase the risk of fungi attack, the shrinkage-swelling phenomenon, and creation of cracks and microcracks, which can in turn influence measured mechanical properties.

**Table 2.** Climatic characteristics of the three environments during the 9 years [28] and moisture content of beam before loading.

| Exposure | Parameters | T (°C) | RH (%) | MC (%) |
|---|---|---|---|---|
| Air-conditioned | Mean | 23.3 | 58.7 | 23 |
| | Standard deviation | 3.2 | 11.4 | - |
| Unsheltered | Mean | 26 | 78 | 23.3 |
| | Standard deviation | 3.8 | 15.1 | - |
| Sheltered outdoor | Mean | 25.3 | 80.8 | 20.7 |
| | Standard deviation | 3.2 | 12.6 | - |

Due to the lack of a climate chamber, the specimens were not conditioned at 12% of moisture content. They were kept in an air-conditioned room where average temperature and relative humidity were 24.3 °C and 43.8, respectively. Since the moisture content is different for each zone (i.e., Table 1), the results of the mechanical tests were adjusted to a moisture content of 12% for comparison purposes by following the procedure indicated in Section 2.2.2.

*2.2. Methods*

2.2.1. Experimental Protocol

The experimental device used for the 3 points bending tests is an 'United' hydraulic press testing system machine of the series N ° 0314523 (Figure 4). The maximum load capacity is 100 kN. The device is connected to a data acquisition system managed by the Datum 5.0 software. The bench test consists of two cylindrical horizontal supports (114.44 mm long and 12.80 mm of diameter). Two small aluminum plates $28.11 \times 8.50 \times 0.41$ mm$^3$ are interposed between the test tube and supports. The test bench is equipped also of a displacement sensor, positioned at the mid-span of the specimen, to measure the arrow. The force increases gradually until the failure of specimen.
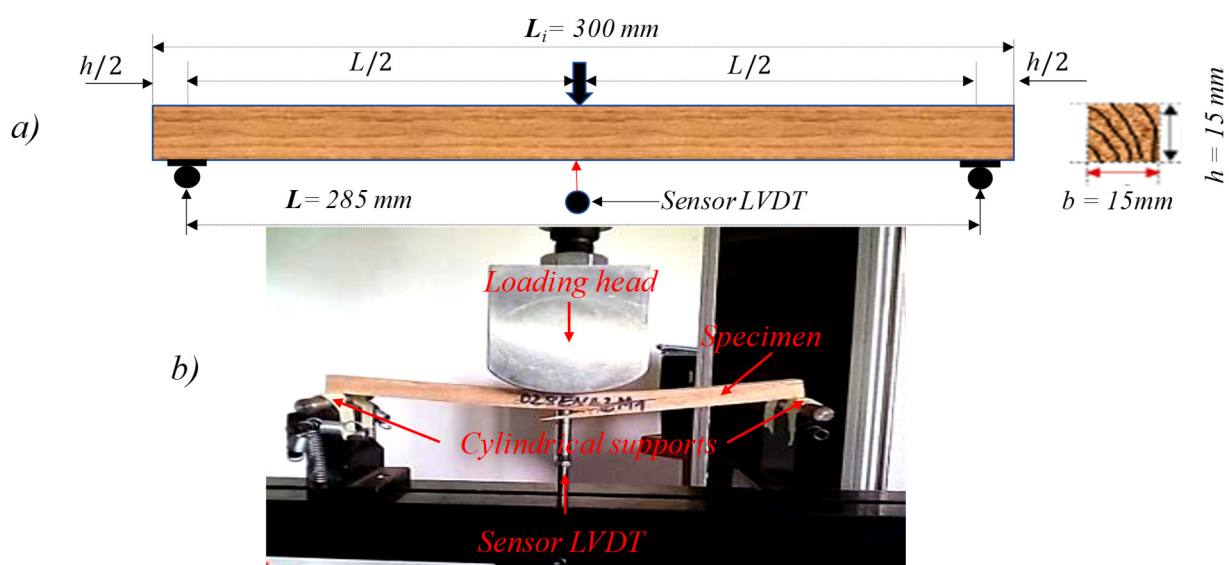


**Figure 4.** (**a**) Three-point bending test bench. (**b**) Experimental device for three-point bending tests.

2.2.2. Assessment of Mechanical Properties

The mechanical tests allow to determine two parameters: failure stress (FS) and Modulus of Elasticity (MOE). The determination of FS is given by Equation (1) [31]:

$$FS = \frac{3 \times \left(F_{max} \times l^3\right)}{2(b \times h^2)},$$ (1)

where $F_{max}$ is the maximum force applied during the bending test, $l$ is the length, $b$ is the thickness and $h$ is the height of the specimen (Figure 4).

The values of MOE (Equation (2)) are obtained according to the NF EN 408 [31] standard:

$$MOE = \frac{l^3 \Delta F}{(b \times h) \times \Delta w},$$ (2)

where $\Delta F$ is the increase in force between 0.1 to $0.4F_{max}$ or 0.2 to $0.3F_{max}$, and $\Delta w$ is the increase in the arrow.

For a comparative study with the results obtained by Manfoumbi [28], the MOE is adjusted to equivalent values for a 12% of moisture content according to NF EN 338 [32] standard by using Equation (3):

$$E_{12\%} = E_W \times [1 - (12 - w) \times 2\%],$$ (3)

where $E_{12\%}$ represents the modulus of elasticity at 12% of the moisture content, and $E_w$ is the modulus of elasticity corresponding to the internal moisture content $w$ of each specimen.

2.2.3. Statistical and Spatial Variability Analyses

The data obtained from experimental tests is statistically analyzed. The statistical analyses are useful to study the effects of environmental conditions on the studied parameters (MC, MOE, and FS) as well as to estimate their correlations. The first stage consists of gathering the data per beam (or exposure type) and to compare the mean, standard deviation, maximum and minimum values, and histograms for each studied parameter. In a second stage, a similar analysis is carried out by gathering data per zone (upper, middle, and lower). In the last stage, the Pearson correlation is computed to estimate the potential correlations between the three studied parameters per environmental condition and zone.

The main goal of the spatial variability analysis is to determine if the database is spatially correlated and stationary. The Ljung–Box (LB) test [33] is performed to examine if autocorrelation exists in this spatial data series. The null hypothesis of the LB test considers that the residuals are independently distributed. Once the existence of the autocorrelation is confirmed by the LB test, the Augmented Dicky Fuller (ADF) test [34] is carried out to determine the stationarity of the spatial data series. The null hypothesis for the ADF test implies that the data series is not stationary.

**3. Results and Discussions**

*3.1. Statistical Analysis of Measured Data*

Figure 5 presents the values of moisture content, modulus of elasticity and failure stress obtained for the three environments for all specimens extracted from the beams (Figure 2). The MOE and FS presented in this figure were adjusted by Equation (3) to consider an equivalent moisture content of 12%. In general, it is observed that all parameters vary for each beam and exposure conditions. Therefore, a statistical analysis will be first carried out to study the influence of the exposure conditions.
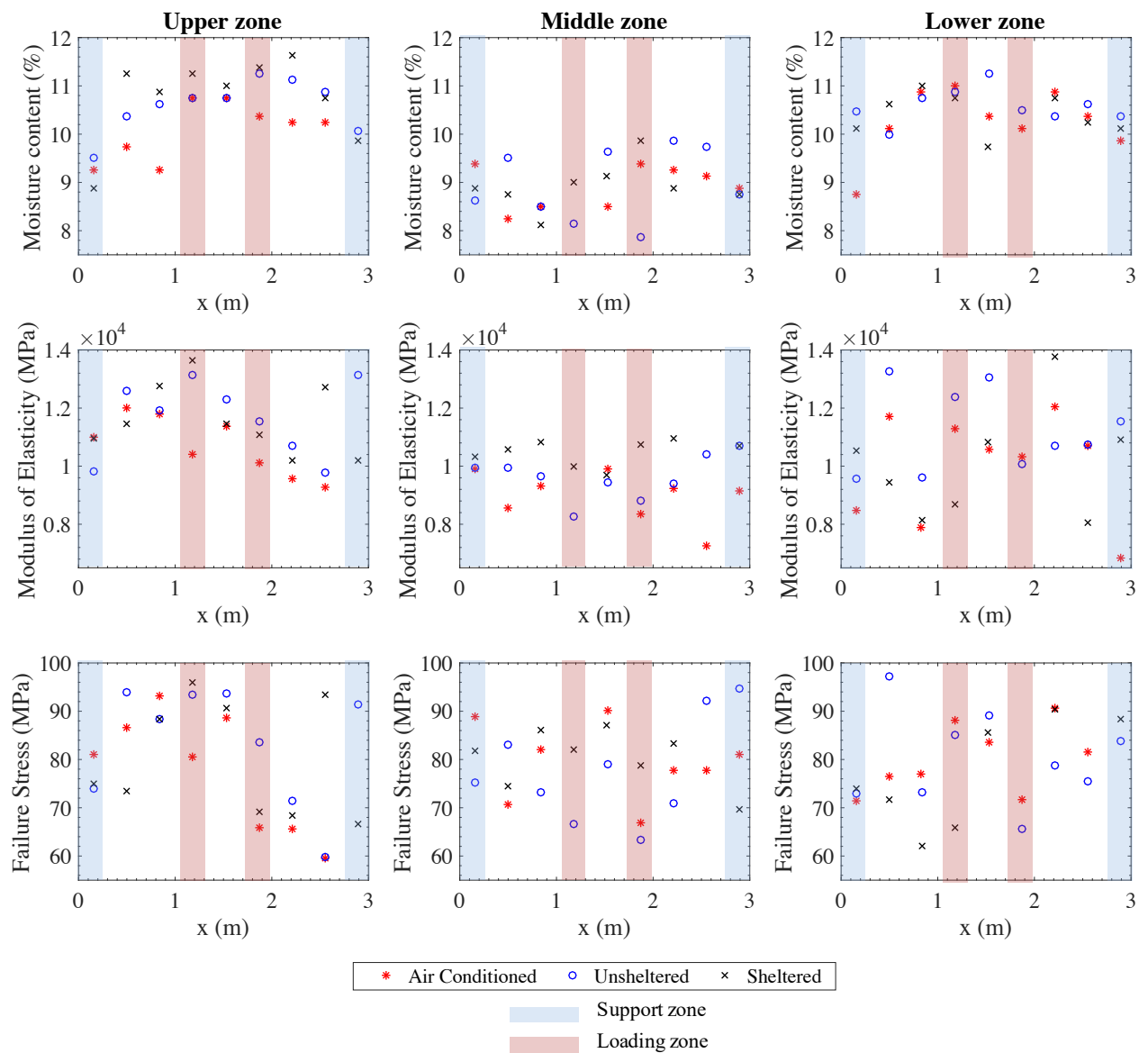
**Figure 5.** Spatial distributed data for the considered parameters and zones.

The data is first gathered per beam/zone and analyzed for each kind of exposure. The histograms for each considered parameter and each beam are summarized in Figure 6. These histograms show different patterns of average values and dispersion of data for each exposure. The mean, standard deviation, and coefficient of variation (CoV) for each exposure/beam/zone are given in Table 3. Concerning moisture content, it is observed that the lower mean value was obtained for the beams under unsheltered exposure. This behavior is due to the fact that the beam was exposed to a dried period before the tests. For the modulus of elasticity and the failure stress, it is noted that higher mean values for beams are estimated for the air-conditioned exposure. This means that the strength of the beam was preserved when it was subjected to controlled environmental conditions. For MOE and FS, the dispersion of the values for the sheltered beams covers almost all the range of the values for air-conditioned and unsheltered exposure conditions (Figure 6).
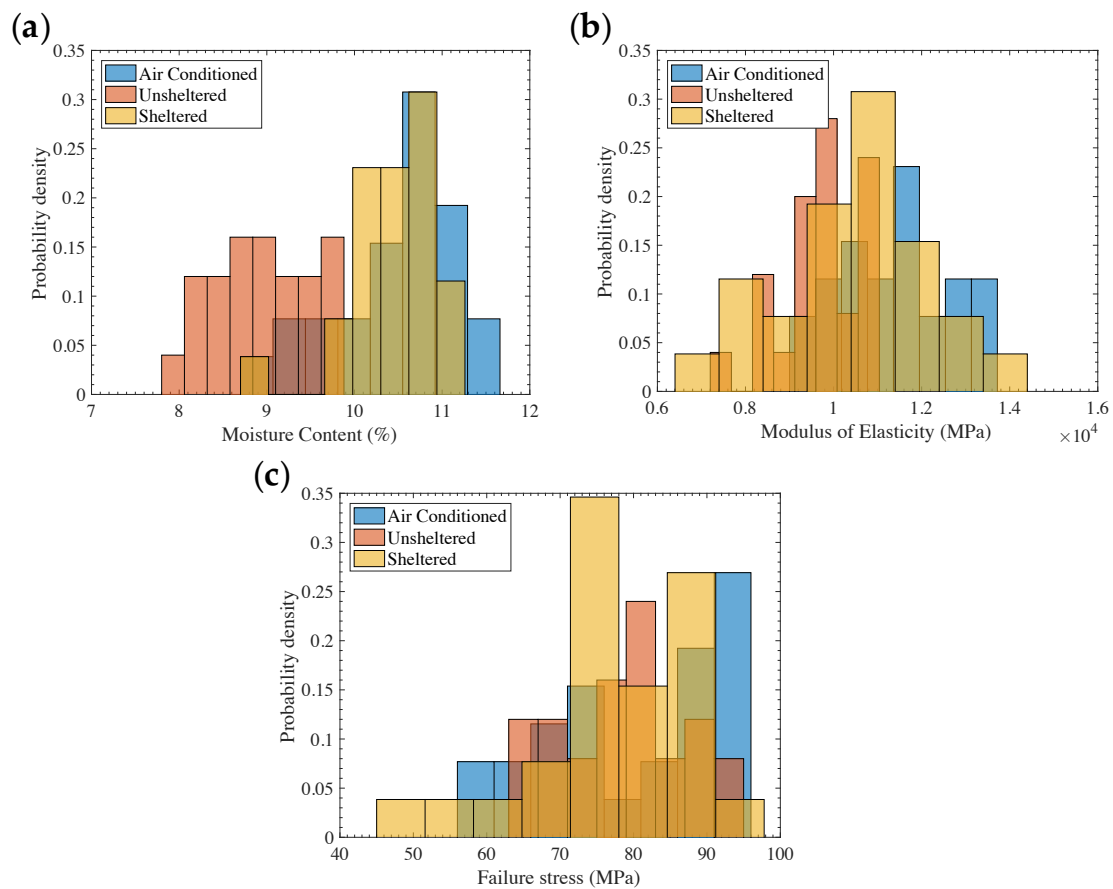
**Figure 6.** Probability densities for each parameter and kind of exposure (**a**) moisture content, (**b**) modulus of elasticity, (**c**) failure stress.

The mean values of the module of elasticity and failure stress are compared to those obtained by Manfoumbi [28] that are also presented in Table 3. The average MOE values were estimated from the instantaneous deflection of the beams measured after loading. The average FS values were computed from samples extracted from the beams but without any differentiation concerning its exposure. For this reason, Table 3 provides the same values for all exposures. It is noted that the mean values of MOE for all beams are lower than that the indicated by Manfoumbi [28]. This decrease of the wood rigidity can be explained by the shrinkage-swelling, creep and mechano-sorptive phenomena, which are more accentuated in environments exposed to the weather than in the air-conditioned environment. Indeed, loss or absence of water in the wood leads to the disappearance of some links [35] such as low-energy (van Der Waals) bonds between water molecules and wood polymers (cellulose, hemicellulose, and lignin); therefore, timber unlinked fibers could be cracked due to water loss. The results obtained partly explain this observation since we observed a very low loss of rigidity (2%) in an air-conditioned environment, compared to sheltered outdoor environments (21%) and unsheltered (35%) in which the surrounding conditions change during the year. Further analysis of the timber microstructure will be very useful to better understand the mechanisms leading to the wood rigidity reduction. Concerning the FS, our values are in average 12 to 16% higher than the reported by Manfoumbi [28]. Nevertheless, the values reported by Manfoumbi [28] are in the range of those found in this work.

Comparing the average values of the parameters in the zones, it is observed in Table 3 that most part of minimum values for each exposure are in the upper zone. Conversely, most maximum values are in the middle zone. The lower zone mainly contains medium average values. Any pattern was identified for the CoV because the range of variation for each zone is not very large. The difference between the zones could be related to the long-term behavior where tensile/compressive stresses reduced the resistance in the

upper/lower zones, respectively. The middle zone, that is normally less loaded, preserving the maximum resistance.

**Table 3.** Mean, standard deviation, maximum and minimum values for each parameter, zone, and kind of exposure.

| Parameter | Exposure | Zone | Mean | St. Dev. | CoV | Min | Max | [28] |
|---|---|---|---|---|---|---|---|---|
| Failure Stress (MPa) | Air conditioned | Upper | 77.63 | 12.42 | 0.17 | 59.58 | 93.3 | – |
| | | Middle | 83.27 | 12.2 | 0.15 | 59.91 | 93.87 | – |
| | | Lower | 80.1 | 11.78 | 0.15 | 67.64 | 95.84 | – |
| | | Beam | 80.4 | 11.9 | 0.15 | 59.6 | 95.8 | 69 |
| | Unsheltered | Upper | 79.41 | 8.04 | 0.1 | 66.94 | 90.15 | – |
| | | Middle | 77.59 | 10.78 | 0.14 | 63.34 | 94.81 | – |
| | | Lower | 80.43 | 5.93 | 0.07 | 69.61 | 87.19 | – |
| | | Beam | 79.1 | 8.3 | 0.1 | 63.3 | 94.8 | 69 |
| | Sheltered | Upper | 76.71 | 12.06 | 0.16 | 49.91 | 90.53 | – |
| | | Middle | 80.12 | 9.66 | 0.12 | 65.5 | 97.17 | – |
| | | Lower | 73.78 | 13.54 | 0.18 | 52.61 | 90.34 | – |
| | | Beam | 77 | 11.6 | 0.15 | 49.9 | 97.2 | 69 |
| Modulus of elasticity (MPa) | Air conditioned | Upper | 10,688 | 1008 | 0.09 | 9283 | 12001 | – |
| | | Middle | 11,662 | 1312 | 0.11 | 9758 | 13,153 | – |
| | | Lower | 11,609 | 1190 | 0.1 | 10,201 | 13,652 | – |
| | | Beam | 11,344 | 1219.7 | 0.11 | 9282.5 | 13,652 | 11,600 |
| | Unsheltered | Upper | 8960 | 878 | 0.1 | 7274 | 9909 | – |
| | | Middle | 9615 | 755 | 0.08 | 8246 | 10,702 | – |
| | | Lower | 10,479 | 508 | 0.04 | 9697 | 10,965 | – |
| | | Beam | 9682.1 | 927 | 10% | 7274.1 | 10,966 | 14,800 |
| | Sheltered | Upper | 9977 | 1816 | 0.18 | 6840 | 12040 | – |
| | | Middle | 11,214 | 1416 | 0.13 | 9 563 | 13257 | – |
| | | Lower | 10,046 | 1888 | 0.19 | 8 075 | 13751 | – |
| | | Beam | 10,427 | 1743 | 17% | 6840.3 | 13,751 | 13,200 |
| Moisture content | Air conditioned | Upper | 10.08 | 0.60 | 0.06 | 9.25 | 10.75 | – |
| | | Middle | 10.59 | 0.55 | 0.05 | 9.5 | 11.25 | – |
| | | Lower | 10.77 | 0.87 | 0.08 | 8.88 | 11.63 | – |
| | | Beam | 10.5 | 0.7 | 7% | 8.9 | 11.6 | – |
| | Unsheltered | Upper | 8.91 | 0.44 | 0.05 | 8.25 | 9.38 | – |
| | | Middle | 8.96 | 0.74 | 0.08 | 7.88 | 9.88 | – |
| | | Lower | 8.92 | 0.49 | 0.05 | 8.125 | 9.875 | – |
| | | Beam | 8.9 | 0.6 | 7% | 7.9 | 9.9 | – |
| | Sheltered | Upper | 10.27 | 0.69 | 0.07 | 8.75 | 11 | – |
| | | Middle | 10.58 | 0.35 | 0.03 | 10 | 11.25 | – |
| | | Lower | 10.42 | 0.42 | 0.04 | 9.75 | 11 | – |
| | | Beam | 10.4 | 0.5 | 5% | 8.8 | 11.3 | – |

The reduction of MOE and FS for the unsheltered and sheltered exposure is due to timber aging, loading duration, and exposure conditions [36–42]. All these parameters considerably influence the resistance of wood due to its nature and anisotropic behavior [43,44]. More particularly, the variations in the moisture content, associated with the exposure and loading, play a key role in the longevity of the wooden structure, because they influence its aging process. The loss of secondary metabolites [45] such as tannins (polyphenols) would also be the cause of decrease in rigidity of the test samples since the tannins act as defender of wood structure by limiting the growth of wood biological agents [46] and the influence of climatic variations (modification of the conformation of molecular structures)

which can alter the main polymers of wood [47]. However, other chemical mechanisms such as the strong crystallization of celluloses [48] in wood can greatly reduce the stiffness of the material. Further analysis of chemical changes will provide additional information allowing to better understand their role on the loss of rigidity.

Determining the potential correlation between the parameters is important when the information will be after used for probabilistic modeling purposes. The Pearson correlations and $p$-values for the studied parameters (MC, MOE, and FS) are given in Table 4. It is noted that the absolute values of the correlations $r_{MC-MOE}$ and $r_{MC-FS}$ are lower than 0.56 with $p$-values larger than 5% for the most part of the cases. This indicates the moisture content is not linearly correlated with the mechanical parameters (MOE and FS). This is explained by the fact that the moisture contents depend on the surrounding weather conditions at the time when the tests were realized. Contrarily, it is possible to state that there is a positive correlation between the mechanical parameters MOE and FS because the values of $r_{MOE-FS}$ are close to 1 with $p$-values lower than 5% for most part of cases. This positive correlation should be considered for propagating uncertainties or spatial variability for these parameters.

**Table 4.** Pearson's correlations and $p$-values for the studied parameters and exposures.

| Exposure | Zone | $r_{MC-MOE}$ | $p$-Value | $r_{MC-FS}$ | $p$-Value | $r_{MOE-FS}$ | $p$-Value |
|---|---|---|---|---|---|---|---|
| Air conditioned | Upper | −0.45 | $2.59 \times 10^{-1}$ | −0.34 | $4.05 \times 10^{-1}$ | 0.94 | $5.38 \times 10^{-4}$ |
| | Middle | 0.05 | $9.05 \times 10^{-1}$ | −0.11 | $7.85 \times 10^{-1}$ | 0.92 | $3.77 \times 10^{-4}$ |
| | Lower | 0.23 | $5.44 \times 10^{-1}$ | 0.16 | $6.87 \times 10^{-1}$ | 0.89 | $1.21 \times 10^{-3}$ |
| Unsheltered | Upper | −0.15 | $7.32 \times 10^{-1}$ | −0.08 | $8.47 \times 10^{-1}$ | 0.69 | $6.07 \times 10^{-2}$ |
| | Middle | 0.46 | $2.11 \times 10^{-1}$ | 0.51 | $1.59 \times 10^{-1}$ | 0.89 | $1.21 \times 10^{-3}$ |
| | Lower | −0.19 | $6.45 \times 10^{-1}$ | −0.09 | $8.26 \times 10^{-1}$ | −0.35 | $4.01 \times 10^{-1}$ |
| Sheltered | Upper | 0.43 | $2.51 \times 10^{-1}$ | 0.56 | $1.15 \times 10^{-1}$ | 0.80 | $9.73 \times 10^{-3}$ |
| | Middle | 0.10 | $7.94 \times 10^{-1}$ | −0.08 | $8.39 \times 10^{-1}$ | 0.92 | $4.25 \times 10^{-4}$ |
| | Lower | −0.18 | $6.64 \times 10^{-1}$ | −0.33 | $4.29 \times 10^{-1}$ | 0.89 | $3.06 \times 10^{-3}$ |

*3.2. Spatial Variability Analysis*

The spatial distribution of the measured parameters given in Figure 5 shows that there exists significant spatial variability for all collected data. The LB test was carried out to confirm the existence of a spatially correlated database. The statistics and $p$-values for the LB test applied to the data obtained in this work are given in Table 5. By considering a significance level of 0.05, it is observed that in all cases the $p$-values are larger than this value confirming that autocorrelation is statistically significant for all spatial data series.

**Table 5.** Statistics and $p$-values (in brackets) for the LB and ADF tests carried out for studied parameters and exposures.

| Exposure | Zone | Moisture Content | | Modulus of Elasticity | | Failure Stress | |
|---|---|---|---|---|---|---|---|
| | | LB | ADF | LB | ADF | LB | ADF |
| Air-conditioned | Upper | 4.96 (0.42) | −0.9 (0.93) | 8.52 (0.12) | −3.25 (0.09) | 10.48 (0.06) | −2.31 (0.45) |
| | Middle | 5.56 (0.35) | 0.59 (0.99) | 3.64 (0.6) | −1.05 (0.91) | 3.65 (0.6) | −2.96 (0.2) |
| | Lower | 1.33 (0.93) | −0.57 (0.96) | 2.65 (0.75) | −32.59 (0.01) | 1.65 (0.89) | −0.62 (0.96) |
| Unsheltered | Upper | 5.11 (0.4) | −0.97 (0.92) | 3.62 (0.6) | −1.56 (0.73) | 5.8 (0.32) | −2.92 (0.22) |
| | Middle | 7.79 (0.16) | −2.93 (0.21) | 8.07 (0.15) | −1.17 (0.88) | 4.24 (0.51) | 10.28 (0.99) |
| | Lower | 4.89 (0.42) | −1.69 (0.68) | 6.65 (0.24) | −2.46 (0.39) | 8.47 (0.13) | 0.25 (0.99) |
| Sheltered | Upper | 2.46 (0.78) | −3.74 (0.03) | 2.22 (0.81) | 2.94 (0.99) | 4.07 (0.53) | −69.92 (0.01) |
| | Middle | 5.02 (0.41) | −1.69 (0.68) | 5.05 (0.4) | −2.26 (0.47) | 7.01 (0.21) | −1.07 (0.9) |
| | Lower | 3.19 (0.67) | −3.02 (0.18) | 1.45 (0.91) | −2.53 (0.36) | 2.42 (0.78) | −3.94 (0.02) |

Figure 5 also shows that there are particular values in the areas of support and application of loads. To better illustrate these particular behaviors, Figure 7 provides the

spatial variability of each parameter estimated by doing an average of the three values per location *x* estimated for upper, middle, and lower zones for each exposure. An average value gathering all measurements (nine values per location *x*) is also shown in this figure (green line). Lower values are observed close to the support zones for the moisture content. This behavior is due to the fact that the beams are more exposed to the environment in the support areas. Some trends with low values of MOE and FS are also observed in the support zone close to 2 m. These trends could be related with the loading conditions that induced more concentrated stresses in these support zones. Since these trends could imply that the spatial variability of the studied parameters is not stationary, statistical tests will be carried out to evaluate the stationarity of these random fields.
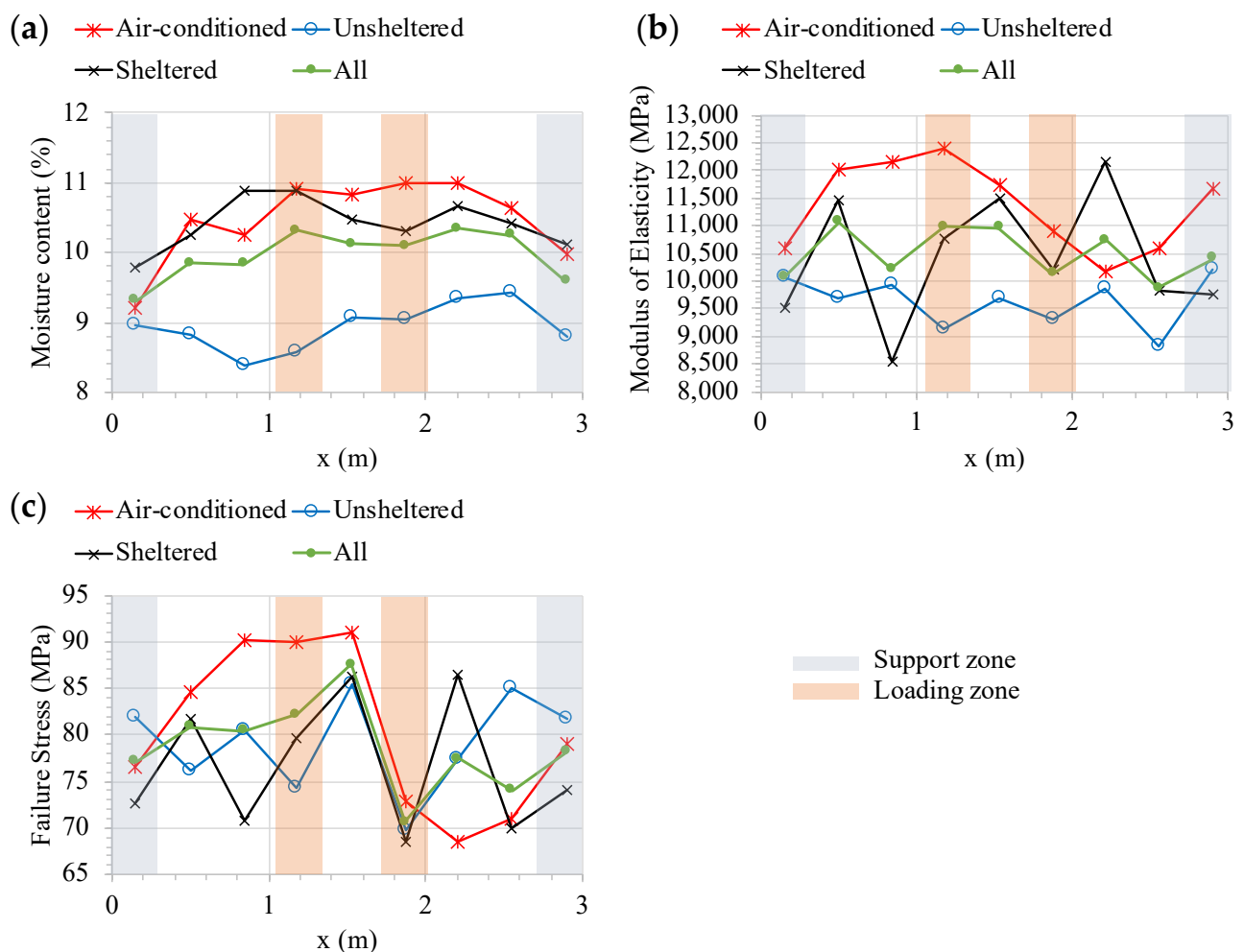


**Figure 7.** Spatial variability of average values of the studied parameters (**a**) moisture content, (**b**) modulus of elasticity, (**c**) failure stress.

The analysis of autocorrelation of a spatial database allows to quantify the spatial regularity of a phenomenon and to determine the extent of the spatial dependence [49]. Figure 8 presents the autocorrelation of the residuals for all beams and exposure conditions. It is observed in all cases that the autocorrelation decreases when the measurements are distant (larger lag #). This suggests that exists a spatial dependency structure [50,51]; however, in several cases, the autocorrelation values are significantly larger/lower than zero indicating a complex autocorrelation structure. Therefore, ADF tests were carried out to confirm the existence of the autocorrelation and to determine if the random fields are stationary. The statistics and *p*-values for the ADF tests are also provided in Table 5. For the same significance level (0.05) the estimated *p*-values indicate that the data series is not

stationary. This result is not surprising considering the trends observed in Figure 7 for the support or loading areas.
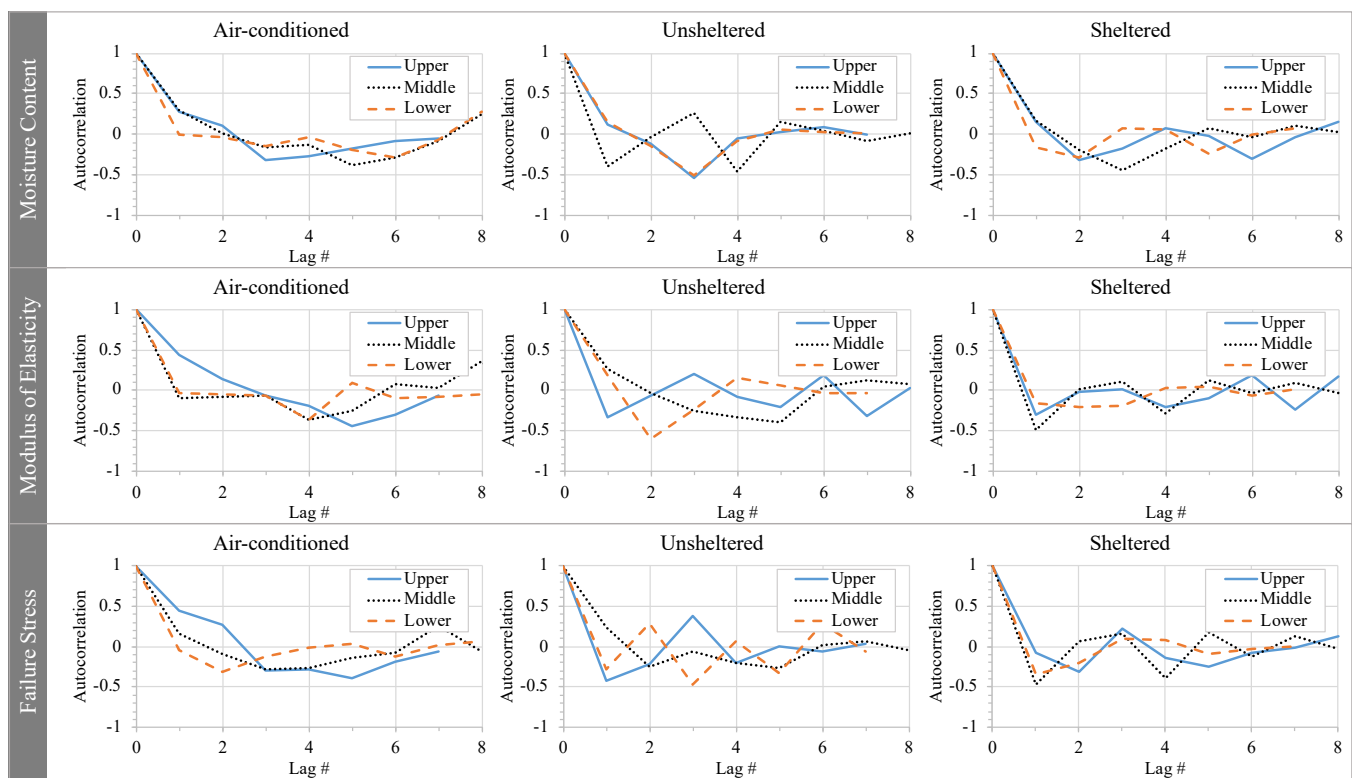


**Figure 8.** Autocorrelation of the studied parameters.

## 4. Conclusions

In this paper, the influence of long-term loading and three exposure conditions on the spatial variability of the moisture content, the modulus of elasticity and the failure of three Ozigo beams are investigated. The results show that the strength of the timber decreases for the specimens exposed to an unsheltered outdoor environment. The strength loss is also larger for the upper and lower zones of the beam than to the middle zone because of the long-term loading. These effects could significantly reduce the service life of timber structures exposed to sheltered and unsheltered outdoor environments. The experimental database allows estimating the correlations between the studied parameters. The correlation analysis showed that the moisture content is not linearly correlated with the modulus of elasticity and the failure stress. However, a positive correlation was estimated between the modulus of elasticity and the failure stress.

In addition, the spatially distributed data was used to study the spatial variability of the studied parameters. First, a LB test statistically confirmed the existence of spatial correlation. Then the spatial distribution of the data and the shapes of the autocorrelation functions suggested that there are some non-stationary trends related to support and loading conditions. This non-stationarity was confirmed by performing the ADF test. These results highlight the importance of the loading and exposure conditions on the spatial variability of the studied materials that induced non-stationarity in the spatial variability. Additional tests on unloaded beams will be very useful to confirm that this non-stationarity is mainly due to loading and support conditions. Future work will also focus on the characterization and then modeling of random fields considering exposure conditions and loading. In addition, the proposed methodology will be applied to other tropical and tempered species. These data and models will ultimately be used for the evaluation and updating of reliability of timber structures by considering spatial variability [27].

According to the impact of long-term loadings on the durability of timbers structures, it is therefore interesting for designers and engineers in the wood construction to consider loading and exposure conditions to improve the durability of timber structures [52–54].

**Abbreviations**

| | |
|---|---|
| $\Delta F$ | Force increment |
| $\Delta w$ | Increase in the arrow |
| $b$ | Thickness of the specimen |
| $E_{12\%}$ | Modulus of elasticity at 12% of the Moisture Content |
| $F_{max}$ | Maximum force |
| FS | Failure Stress |
| $h$ | Height of the specimen |
| $l$ | Length of the specimen |
| LZ | Lower zone |
| MC | Moisture Content |
| MOE | Modulus of elasticity |
| MZ | Middle zone |
| RH | Relative humidity |
| T | Temperature |
| UZ | Upper zone |
| $E_w$ | Modulus of elasticity corresponding to the Moisture Content |
| $w$ | Internal moisture content of each specimen |

## References

1. Bayol, N.; Anquetil, F.; Bile, C.; Bollen, A.; Bousquet, M.; Castadot, B.; Meunier, Q. Timber industry and natural forest management: Tropical timber and central African forests in the face of market developments. *For. Congo Basin State For.* **2013**, *2013*, 47–66.
2. Ikogou, S.; Pambou Nziengui, C.F.; Moutou Pitti, R.; Ekomy Ango, S. Experimental study of tropical wood under cyclic compressive loading for sustainable constructions. In Proceedings of the World Conference of Timber Engineering (WCTE), Vienna, Austria, 22–25 August 2016.
3. Allan, K.; Phillips, A. Comparative Cradle-to-Grave Life Cycle Assessment of Low and Mid-Rise Mass Timber Buildings with Equivalent Structural Steel Alternatives. *Sustainability* **2021**, *13*, 3401. [CrossRef]
4. Tahmasebinia, F.; Ma, Y.; Joshua, K.; Sepasgozar, S.; Yu, Y.; Li, J.; Sepasgozar, S.; Marroquin, F. Sustainable Architecture Creating Arches Using a Bamboo Grid Shell Structure: Numerical Analysis and Design. *Sustainability* **2021**, *13*, 2598. [CrossRef]
5. Pambou Nziengui, C.F.; Ikogou, S.; Moutou Pitti, R. Impact of cyclic compressive loading and moisture content on the me-chanical behavior Aucoumea Klaineana Pierre. *Wood Mater. Sci. Eng.* **2017**, *13*, 190–196. [CrossRef]
6. Grubben, G.J.H.; Denton, O.A. *Plan Ressources of Tropical Africa, Timbers 1*; Backhuys Publishers: Leiden, The Netherlands, 2008; pp. 203–204.

7.  Tran, T.-B.; Bastidas-Arteaga, E.; Aoues, Y.; Nziengui, C.P.; Hamdi, S.; Pitti, R.M.; Fournely, E.; Schoefs, F.; Chateauneuf, A. Reliability assessment and updating of notched timber components subjected to environmental and mechanical loading. *Eng. Struct.* **2018**, *166*, 107–116. [CrossRef]
8.  Pambou Nziengui, C.F. Cracking of Wood in Variable Climate under Long-Term Loads: Applications to European and Gabo-nese Species. Ph.D. Thesis, Clermont Auvergne University, Clermont-Ferrand, France, 2019.
9.  Chassagne, P.; Saïd, E.B.; Jullien, J.F.; Galimard, P. Three Dimensional Creep Model for Wood under Variable Humidity-Numerical Analyses at Different Material Scales. *Mech. Time-Dependent Mater.* **2005**, *9*, 1–21. [CrossRef]
10. Pittet, V. Experimental Study of Mechanosorptive Couplings in Wood Subjected to Controlled Hygrometric Variations under Long Duration Loadings. Ph.D. Thesis, Ecole Polytechnique Federal de Lausanne, Lausanne, Switzerland, 1996.
11. Saifouni, O. Modeling of Rheological Effects in Materials: Application to the Mechanosorptive Behavior of Wood. Solid Me-chanics. Ph.D. Thesis, Blaise Pascal University, Clermont-Ferrand, France, 2014.
12. Toratti, T.; Morlier, P. Long-term creep of bent wood in structural size. *Mater. Struct.* **1995**, *28*, 284–292. [CrossRef]
13. Moshtaghin, A.F.; Franke, S.; Keller, T.; Vassilopoulos, A.P. Experimental characterization of longitudinal mechanical properties of clear timber: Random spatial variability and size effects. *Constr. Build. Mater.* **2016**, *120*, 432–441. [CrossRef]
14. Natterer, J.; Sandoz, J.-L.; Rey, M. *Wood Construction: Materials, Technology and Sizing*; Edition Presses Polytechniques and Universitaires Romandes, Civil Engineering Treaty: Lausanne, Switzerland, 2004; p. 13.
15. Vořechovský, M. Interplay of size effects in concrete specimens under tension studied via computational stochastic fracture mechanics. *Int. J. Solids Struct.* **2007**, *44*, 2715–2731. [CrossRef]
16. Sriramula, S.; Chryssanthopoulos, M.K. An experimental characterisation of spatial variability in GFRP composite panels. *Struct. Saf.* **2013**, *42*, 1–11. [CrossRef]
17. Ravahatra, N.R.; Duprat, F.; Schoefs, F.; De Larrard, T.; Bastidas-Arteaga, E. Assessing the Capability of Analytical Carbonation Models to Propagate Uncertainties and Spatial Variability of Reinforced Concrete Structures. *Front. Built Environ.* **2017**, *3*, 1–9. [CrossRef]
18. Clerc, R.; Oumouni, M.; Schoefs, F. SCAP-1D: A Spatial Correlation Assessment Procedure from unidimensional discrete data. *Reliab. Eng. Syst. Saf.* **2019**, *191*, 106498. [CrossRef]
19. Ravahatra, N.R.; Bastidas-Arteaga, E.; Schoefs, F.; Duprat, F.; De Larrard, T.; Oumouni, M. Characterisation and propagation of spatial fields in deterioration models: Application to concrete carbonation. *Eur. J. Environ. Civ. Eng.* **2019**, 1–27. [CrossRef]
20. Li, C.; Der Kiureghian, A. Optimal Discretization of Random Fields. *J. Eng. Mech.* **1993**, *119*, 1136–1154. [CrossRef]
21. Loève, M. *Probability Theory*, 4th ed.; Springer: New York, NY, USA, 1977.
22. Ghanem, R.G.; Spanos, P.D. Spectral Stochastic Finite-Element Formulation for Reliability Analysis. *J. Eng. Mech.* **1991**, *117*, 2351–2372. [CrossRef]
23. Sudret, B.; Der Kiureghian, A. *Stochastic Finite Elements and Reliability: A State-of-the-Art Report. Report No: UCB/SEMM-2000/08*; Department of Civil & Environmental Engineering-University of California: Berkeley, CA, USA, 2000.
24. Stewart, M. Spatial variability of damage and expected maintenance costs for deteriorating RC structures. Structure & Infra-structure Engineering: Maintenance, Management. *LifeCycle Design Perform.* **2006**, *2*, 70–90.
25. Zhu, F.; Zhou, Q.; Wang, F.; Yang, X. Spatial variability and sensitivity analysis on the compressive strength of hollow concrete block masonry wallettes. *Constr. Build. Mater.* **2017**, *140*, 129–138. [CrossRef]
26. Moshtaghin, A.F.; Franke, S.; Keller, T.; Vassilopoulos, A.P. Random field-based modeling of size effect on the longitudinal tensile strength of clear timber. *Struct. Saf.* **2016**, *58*, 60–68. [CrossRef]
27. Tran, T.-B.; Bastidas-Arteaga, E.; Aoues, Y. A Dynamic Bayesian Network framework for spatial deterioration modelling and reliability updating of timber structures subjected to decay. *Eng. Struct.* **2020**, *209*, 110301. [CrossRef]
28. Manfoumbi Boussougou, N. Contribution to the Adaptation of Eurocode 5 to Tropical Hardwoods in Their Environment. Ph.D. Thesis, University if Limoges, Limoges, France, 2012.
29. Gérard, J.; Beauchêne, J.; Fouquet, D.; Guibal, D.; Langbour, P.; Thévenon, M.-F.; Thibaut, A.; Vernay, M. *TROPIX 5.0: Technological Characteristics of 215 Tropical Species*; CIRAD Forest Department: Montpellier, France, 2011.
30. Meunier, Q.; Moumbogou, C.; Doucet, J.-L. *Useful trees in Gabon*; Gembloux Agricultural Press: Gembloux, Belgium, 2015; p. 116.
31. *NF EN 408 Timber Structures-Structural Timber and Glued Laminated Timber. Determination of Certain Physical and Mechanical Properties*; AFNOR: Saint-Denis, France, 2009.
32. *NF EN 338 Structural Timber-Strength Classes*; AFNOR: Saint-Denis, France, 2009.
33. Ljung, G.M.; Box, G.E.P. On a measure of lack of fit in time series models. *Biomertrika* **1978**, *65*, 297–303. [CrossRef]
34. Banerjee, A.; Dolado, J.J.; Galbraith, J.W.; Hendry, D. *Co-Integration, Error Correction, and the Econometric Analysis of Non-Stationary Data*; Oxford University Press (OUP): Oxford, UK, 1993.
35. Gfeller, B.; Zanetti, M.; Properzi, M.; Pizzi, A.; Pichelin, F.; Lehmann, M.; Delmotte, L. Wood bonding by vibrational welding. *J. Adhes. Sci. Technol.* **2003**, *17*, 1573–1589. [CrossRef]
36. Husson, J.M. Elastic Behavior Law with Memory Effect. Ph.D. Thesis, University of Limoges, Limoges, France, 2009.
37. Armstrong, L.D.; Kingston, R.S.T. Effet of moisture changes on creep in wood. *Nature* **1960**, *185*, 862–863. [CrossRef]
38. Brancheriau, L.; Baillères, H.; Guitard, D. Comparison between modulus of elasticity values calculated using 3 and 4 point bending tests on wooden samples. *Wood Sci. Technol.* **2002**, *36*, 367–383. [CrossRef]

39.  Houanou, A.K.; Tchéhouali, A.D.; Foudjet, A.E. Effect of the loading duration on the linear viscoelastic parameters of tropical wood: Case of Tectona grandis L.f (Teak) and Diospyros mespiliformis (Ebony) of Benin Republic. *SpringerPlus* **2014**, *3*, 74. [CrossRef] [PubMed]
40.  Karlinasari, L.; Wabyuna, M.E.; Nugroho, N. Non-destructive ultrasonic testing method for determining bending strength properties of Gmelina wood (Gmelina arborea). *J. Trop. For. Sci.* **2008**, *20*, 99–104.
41.  Ravenshorst, G.J.P.; Van De Kuilen, J.W.G.; Brunetti, M.; Crivellaro, A. Species independent machine stress grading of hardwoods. In Proceedings of the 10th world conference on timber engineering (WCTE), Miyazaki, Japan, 2–5 June 2008.
42.  Teles, R.; Del Menezzi, C.; Souza, F.; Souza, M. Nondestructive Evaluation of a Tropical Hardwood: Interrelationship Between Methods and Physical-Acoustical Variables. *Rev. Ciência Madeira RCM* **2011**, *2*, 1–14. [CrossRef]
43.  Bodig, J.; Jayne, B.A. *Mechanics of Wood and Wood Composites*; Van Nostrand Reinhold: New York, NY, USA, 1982.
44.  Tsoumis, G. *Science and Technology of Wood: Structure, Properties, Utilization*; Chapman & Hall: New York, NY, USA, 1991; p. 11.
45.  Athomo, A.B.B.; Anris, S.P.E.; Tchiama, R.S.; Leroyer, L.; Pizzi, A.; Charrier, B. Chemical analysis and thermal stability of African mahogany (Khaya ivorensis A. Chev) condensed tannins. *Holzforschung* **2020**, *74*, 683–701. [CrossRef]
46.  Brunck, F. Parasites des plantations forestières d'Afrique Tropicale et Madagascar et mesure de protection. *Bois Forêts Tropiques* **1965**, *103*, 17–25.
47.  John, M.J.; Anandjiwala, R.D. Recent developments in chemical modification and characterization of natural fiber-reinforced composites. *Polym. Compos.* **2008**, *29*, 187–207. [CrossRef]
48.  Pizzi, A.; Cameron, F.A. Flavonoid tannins-structural wood components for drought-resistance mechanisms of plants. *Wood Sci. Technol.* **1986**, *20*, 119–124.
49.  Aubry, P.; Piégay, H. Pratique de l'analyse de l'autocorrélation spatiale en géomorphologie: Définitions opératoires et tests. *Géographie Phys. Quat.* **2001**, *55*, 111–129. [CrossRef]
50.  Gatrell, A.C. Autocorrelation in Spaces. *Environ. Plan. A Econ. Space* **1979**, *11*, 507–516. [CrossRef]
51.  Cliff, A.D.; Ord, J.K. *Spatial Processes: Models and Applications*; Pion: London, UK, 1981; p. 266.
52.  Mvondo, R.R.N.; Meukam, P.; Jeong, J.; Meneses, D.D.S.; Nkeng, E.G. Influence of water content on the mechanical and chemical properties of tropical wood species. *Results Phys.* **2017**, *7*, 2096–2103. [CrossRef]
53.  Madsen, B. *Structural Behaviour of Timber*; Timber Engineering Ltd.: Vancouver, Canada, 1992; p. 437.
54.  Wood, L.W. Behaviour of wood under continued loading. *Eng. News Record.* **1947**, *139*, 108–111.